Author Manuscript

Author Manuscript

Author Manuscript

Author Manuscript

HHS Public Access

Author manuscript

J Biomed Mater Res B Appl Biomater. Author manuscript; available in PMC 2018 April 01.

Published in final edited form as:

J Biomed Mater Res B Appl Biomater. 2017 April ; 105(3): 560–567. doi:10.1002/jbm.b.33578.

Preparation, characterization and in vitro response of bioactive coatings on polyether ether ketone

John W. Durham III[1], **Matthew J. Allen**[1], and **Afsaneh Rabiei**[2]

[1]Department of Mechanical and Aerospace Engineering, North Carolina State University, Raleigh, North Carolina 27695

[2]Department of Veterinary Medicine, University of Cambridge, Cambridge, United Kingdom

Abstract

Polyether ether ketone (PEEK) is a highly heat-resistant thermoplastic with excellent strength and elastic modulus similar to human bone, making it an attractive material for orthopedic implants. However, the hydrophobic surface of PEEK implants induces fibrous encapsulation which is unfavorable for stable implant anchorage. In this study, PEEK was coated via ion-beam-assisted deposition (IBAD) using a two-layer design of yttria-stabilized zirconia (YSZ) as a heat-protection layer, and hydroxyapatite (HA) as a top layer to improve osseointegration. Microstructural analysis of the coatings showed a dense, uniform columnar grain structure in the YSZ layer and no delamination from the substrate. The HA layer was found to be amorphous and free of porosities in its as-deposited state. Subsequent heat treatment via microwave energy followed by autoclaving crystallized the HA layer, confirmed by SEM and XRD analysis. An in vitro study using MC3T3 preosteoblast cells showed improved bioactivity in heat-treated sample groups. Cell proliferation, differentiation, and mineralization were analyzed by MTT assay and DNA content, osteocalcin expression, and Alizarin Red S (AR-S) content, respectively. Initial cell growth was increased, and osteogenic maturation and mineralization were accelerated most on coatings that underwent a combined microwave and autoclave heat treatment process as compared to uncoated PEEK and amorphous HA surfaces.

Keywords

bioactive coatings; hydroxyapatite; PEEK; physical vapor deposition; crystallinity

INTRODUCTION

The success and lifetime of orthopedic implants rely on a number of factors, arguably the most important being the interaction between the body and the orthopedic device. Implant failure can be characterized by the need for revision surgeries, which are well documented and often necessary because of device loosening or lack of bone apposition.[1] Ideally an implant is designed to closely mimic the biological tissue that it is replacing, in order to provide structural stability and support bone growth. This can be achieved by matching the

Correspondence to: A. Rabiei; arabiei@ncsu.edu.

Author Manuscript Author Manuscript Author Manuscript Author Manuscript

tissue's mechanical properties as well as its surface chemistry. However, this has been a difficult challenge due to the lack of available engineering materials and fabrication methods. Advances in material science have changed the way we approach such constraints, offering a much larger range of options than ever before.[2]

In the past few decades, some polymers have proven to better match the mechanical properties of human bone and have become accepted alternatives to traditional metallic implant materials in several applications.[2,3] Engineered polymer materials have the potential to reduce stress-shielding and bone loss, contributing to improved patient outcomes.[2] In particular, polyether ether ketone (PEEK) has become an attractive orthopedic material because of its heat resistance, excellent strength, and elastic modulus closely matching human bone.[3,4] PEEK is also radiolucent when examined by plain film radiography, computed tomography, or magnetic resonance imaging, a property that is particularly useful when the primary intent of such imaging modalities is to examine the healing response of peri-implant tissues. In addition, PEEK is suitable for most sterilization techniques such as gamma irradiation, ethylene oxide, or autoclave due to its chemical inertness and stability.[5]

PEEK biomaterials are now used in a variety of medical applications, and are especially popular in spinal implant procedures.[6,7] Interbody spinal fusion is a common procedure performed to treat lower back problems, in which an implantable rectangular cage is used as a spacer between adjacent vertebrae with the intent to fuse them together. Unfortunately, pseudoarthrosis—failure of the device to fuse after the procedure—still occurs in 20–40% of cases.[8] The inert hydrophobic surface of PEEK implants can induce fibrous encapsulation that impedes bone apposition, making fusion difficult.[9] One potential solution is to alter the implant surface chemistry by coating PEEK with a thin bioactive calcium phosphate coating surface then mimics the adjacent bone tissue and encourages bone apposition.

The traditional method for preparing such coatings on metallic implants is plasma spraying, a deposition process involving high temperatures that can damage thermoplastic substrates such as PEEK. Plasma-sprayed coatings also lack strong adhesion to their substrate, material homogeneity, and mechanical robustness.[10] Other coating methods have been investigated with varying degrees of success,[11–13] though a standard practice has yet to emerge.

In a previous study, a two-layer coating was developed, consisting of yttria-stabilized zirconia (YSZ) as a heat-protection layer over PEEK, and an HA top layer for improved biocompatibility. Physical vapor deposition via radiofrequency (RF) magnetron sputtering was used to deposit such films on PEEK and resulted in improved substrate adhesion compared to traditional coating techniques.[14] An effective heat treatment was then used to crystallize the HA layer after deposition; crystalline HA exhibits superior dissolution rates *in vitro* and *in vivo* compared to amorphous HA. The coatings were heat treated by unconventional methods to address the incompatibility of PEEK with typical HA sintering temperatures.[15] Briefly, microwave heat treatment allows for selective energy absorption and volumetric heating in dielectric materials like HA while microwave-transparent materials like PEEK experience small absorption. Additional autoclave treatment can further crystallize HA by substituting conventional high-temperature treatment with moderate

Author Manuscript Author Manuscript Author Manuscript Author Manuscript

temperatures and elevated pressure.[16] These heat treatment processes are described in further detail in our previous study.[14]

The work described here builds upon these findings to further improve the process by implementing ion-beam assisted deposition (IBAD) of YSZ and HA on PEEK. The IBAD is capable of higher deposition rates with increased coating density and adhesion due to secondary ion bombardment and atomic mixing at the interfacial zone. Previous studies have reported deposition of a dense, functionally graded HA coating on titanium via IBAD by controlling substrate temperature.[17,18] This work uses the IBAD method to deposit a two-layer HA/YSZ coating on PEEK. Following deposition, a combination of heat treatment via microwave followed by autoclave treatment was used to enhance the crystallinity and bioactivity of the HA coating at subthreshold temperatures for PEEK. The as-deposited and heat-treated coatings were characterized by SEM, XRD, and FTIR. *In vitro* evaluation was then performed to determine the effects of the different treatments on the proliferation, survival, and biological function of osteoblasts cultured on the surface of treated discs.

MATERIALS AND METHODS

Substrate preparation

Flat discs of ¼-inch height cut from a ½-inch diameter PEEK rod (PEEK-OPTIMA®, Invibio Ltd. Technology, Lancashire, United Kingdom) using a lathe-mounted parting tool. For batch processing, discs were mounted to a grinding plate using an inert, dissolvable wax adhesive. The discs were then wet-ground sequentially against 180, 320, 400, and 600-grit silicon carbide article (Buehler) using an automated grinding station (Buehler) with deionized water rinsing between steps. The discs were removed and ultrasonically cleaned for 10 min cycles with acetone (3×), isopropanol, and deionized water, respectively. The substrates were dried using compressed air and stored in sterile culture plates prior to deposition.

Surface activation

Prior to deposition, the PEEK substrate surfaces underwent a brief surface treatment via O_2 plasma treatment in a radiofrequency plasma barrel reactor (PM-600, March Instruments) for 20 min. Substrate discs were then transferred to the IBAD system chamber for deposition. Uncoated PEEK samples representing commercial PEEK implants did not undergo plasma treatment and used as is.

Coating deposition

Deposition of YSZ and HA was achieved using an IBAD system (Univex 600, Oerlikon Leybold Vacuum) consisting of an 8″ target, and 6″ substrate deposition area. Substrates were held in place using a perforated mounting fixture fabricated from commercially pure titanium to avoid potential coating contamination caused by surface resputtering. The 16-cm primary and 12-cm secondary ion sources use argon process gas (Figure 1). Substrate table rotation was used to produce uniform film thickness across the sample batch. The ion source deposition parameters were optimized for film thickness and density. The base vacuum pressure achieved before deposition was approximately 5×10^{-7} Torr and deposition

Author Manuscript Author Manuscript Author Manuscript Author Manuscript

pressure varied from 3 to 5×10^{-4} Torr depending on the primary and secondary ion source flow rates. The deposition temperature was monitored and maintained well below the glass transition temperature of PEEK to avoid any damage to the polymer substrate during deposition. The deposition chamber was vented to atmospheric conditions between the YSZ and HA layer deposition in order to perform the target exchange.

X-ray diffraction—Chemical surface composition and crystalline phases of the deposited and heat-treated coatings were determined by X-ray diffraction (SmartLab®, Rigaku) with Cu Kα source at 40 kV and 44 mA. Scans were performed between 20° and 40° 2θ at a rate of 0.5°/min and in glancing angle mode (0.5° incident angle), ideal for surface analysis. A small portion of the HA target was used to verify the bulk material spectrum before deposition for comparative analysis. Powder diffraction standards (JCPDS) using PDXL software were used to identify and confirm crystalline YSZ and HA phase peaks.

Scanning electron microscopy

The microstructure and surface morphology of the deposited and heat-treated films were observed by scanning electron microscopy (SEM) using a high-resolution field emission SEM (FEI, Verios 460 L).

Fourier transform infrared spectroscopy

Analysis of surface molecular chemistry was determined by Fourier transform infrared spectroscopy (FTIR) using a Thermo-Nicolet Nexus 470 configured with a beryllium attenuated total reflectance (ATR) insert. A small portion of the HA target was again used to obtain FTIR spectrum for the bulk material.

Postdeposition heat treatment

The HA/YSZ coatings on PEEK were processed via two heat treatment methods following deposition. Selective heating of the coating was achieved with the use of a variable frequency microwave oven (Microcure, Lambda Technologies) in order to aid in crystallization of the HA layer without damaging the underlying PEEK substrate. The microwave unit delivers power up to 400 W at a frequency range of 5.8–7 GHz to perform the heat treatment in accordance with the methods described in patent US8323722.[19]

Autoclave processing was also applied to the samples using a commercial sterilization unit (Prevac Steam Sterilizer, Steris). The temperature-programmable autoclave was adjusted to apply a saturated steam cycle of 136°C for 8 h; time and temperature were optimized with respect to crystallinity.

Biocompatibility analysis

The cell culture study consisted of four experimental groups: (1) uncoated PEEK (PEEK); (2) as-deposited HA/YSZ coating on PEEK (AD); (3) as-deposited HA/YSZ coating on PEEK with autoclave treatment (AD + AC); (4) HA/YSZ coating on PEEK followed by microwave annealing and autoclave treatment (MW + AC). A total of 240 samples (60 per group) were then sterilized in ethylene oxide and vented for at least 72 h to ensure complete

Author Manuscript Author Manuscript Author Manuscript Author Manuscript

elimination of residuals prior to use in the cell culture study. Tissue culture-treated polystyrene (TCPS) served as the negative control for the cell culture testing.

Cell line and growth

Murine MC3T3 osteoblasts were maintained in minimum essential medium alpha (α-MEM) supplemented with 10% fetal calf serum and 1% antibiotics. Cells were cultured at 37°C in an atmosphere of 5% CO_2 in air. Separately, samples were placed in 24-well tissue culture plates, prewetted with 500 μL of complete α-MEM containing 10% fetal calf serum and incubated at 37°C for 60 min. The medium was then removed and cells (5×10^4) suspended in a volume of 200 μL of α-MEM were then seeded onto the sample surfaces and incubated for at least 10 min at 37°C to allow them to settle on the sample surface. An additional 1 mL of pre-warmed medium was added, covering the samples by several millimeters. Plates were then incubated at 37°C in a humidified atmosphere containing 5% CO2 in air and the medium was removed and replaced 2–3 times per week for the duration of the experiment.

Cell proliferation

The growth of MC3T3 cells on each sample group was compared with growth on TCPS, an established control material. Cell proliferation was measured using MTT reagent (MTT) at 1, 2, and 3 days. In brief, MTT solution (5 mg/mL) was added to 4 wells per test item; after a 60 min incubation, the medium was removed, the cells rinsed in phosphate-buffered saline (PBS) and then lysed in 500 μL of dimethyl sulfoxide (DMSO). The optical density of the resultant solution, measured at a wavelength of 562 nm is proportional to the number of viable cells in the culture well.

Measurement of total DNA content—The DNA content was measured at 14 and 21 days postseeding. At each time point, the medium was removed from test and control wells and the adherent cells lysed by repeated freeze–thaw cycles in Tris–EDTA buffer. The concentration of DNA in the sample was then measured using a commercial assay for double-stranded DNA (AccuBlue™ dsDNA Quantitation Kit; Cambridge Bioscience, Cambridge, UK).

Osteoblastic differentiation

Osteocalcin (OC), an established marker of a mature osteoblast, was measured at 14 and 21 days postseeding. Quantification of OC levels in the medium was performed by enzyme-linked immunoabsorbent assay (ELISA). The data was then normalized to the DNA content of the corresponding cell lysate.

Osteoblastic mineralization

For the mineralization study, cells were seeded on the samples and the TCPS control as described previously. As soon as the cultures appeared confluent, the medium was switched to mineralizing medium: α-MEM plus 10% FCS supplemented with 50 μg/mL ascorbic acid and 4 mM sodium phosphate. Media were changed twice weekly for 3 weeks. At the end of the study period, medium was removed, test and control were rinsed three times in PBS, and the monolayer was fixed in ice-cold 70% alcohol for 60 min. The fixed monolayer was then

Author Manuscript Author Manuscript Author Manuscript Author Manuscript

stained with Alizarin Red S (AR-S) (40 mM, pH 4.2) for 10 min, rinsed five times in PBS, and the bound AR-S eluted through disruption of the cell monolayer with cetylpyridinium chloride (10% w/v in sodium phosphate, pH 7.0). Eluted AR-S was quantified by spectrophotometry at 562 nm.

Statistical analysis

Comparisons between the sample groups were made using a one-way analysis of variance (ANOVA) at individual time points. Post-hoc Tukey tests were then used as appropriate to determine intergroup differences. A significance level of $p < 0.05$ was used in all analyses.

RESULTS

Microstructural analysis

Figure 2 shows the cross-section of the HA/YSZ coatings via SEM including AD, AD + AC, and MW + AC samples. Measurement of the coatings show a 2-μm-thick coating was successfully deposited on PEEK comprised of a 1-μm YSZ bottom layer and 1-μm HA top layer. The SEM results in conjunction with the IBAD process times indicate a deposition rate of ~250 nm/h for both YSZ and HA. Close observation of the cross-section shows that the IBAD-deposited coatings are highly dense and uniform, with no visible porosities. The PEEK/YSZ interface shows no delamination, suggesting a strong bond between the coating and the substrate. A crystalline YSZ structure composed of columnar grains oriented normal to the substrate surface was seen in all sample groups. The HA layer appeared to be amorphous in its as-deposited state from Figure 2(a). The MW + AC sample in Figure 2(c) shows an enhanced crystalline structure throughout the coating thickness while the AD + AC sample exhibited a small region of crystalline morphology near the top and bottom of the HA layer [Figure 2(b)]. These results are in agreement with our previous observations reported elsewhere.[14]

Compositional analysis

XRD spectra were obtained to determine the chemical composition and crystalline phases present in the coating. The underlying PEEK spectrum was not observed due to the glancing angle configuration and only the coating spectrum is present. As seen in Figure 3, all coated sample types exhibited crystalline YSZ peaks for (1 0 1) and (1 1 0) phases. The spectrum of the as-deposited coating did not show any crystalline HA peaks, indicating an amorphous structure. However, the heat-treated samples show increased crystallinity evident by the appearance of crystalline HA (0 0 2), (2 1 1), and (3 0 0) phases in the AD + AC and MW + AC spectra. Measurement of the 2θ peak positions obtained from these spectra closely matched those observed in the bulk target material and the JCPDS standard HA peak positions.

Fourier transform infrared spectroscopy

Figure 4 shows the FTIR spectra of the coated sample types and the HA target. The HA target shows a strong absorption peak at approximately 1084 cm^{-1} and a sharp, lower intensity peak at ~3650 cm^{-1}, corresponding to the phosphate and hydroxyl groups of crystalline HA, respectively. The coated samples all exhibit strong phosphate absorption

Author Manuscript Author Manuscript Author Manuscript Author Manuscript

peaks, but lack the hydroxyl peak, showing only a broad signal in the general OH^- region in the spectra. This indicates that the HA target material was dehydroxylated during the deposition process as the coating was applied, which has been previously observed in vacuum sputtering techniques.[20]

Biological response

MTT is used as a marker of viable cell numbers within a growing culture. Figure 5 shows the comparison of the coated samples with the uncoated PEEK as the control. A general trend of increasing cell growth rate was observed for all coated groups with increasing cell culture period. Cell numbers were significant higher (relative to the control) for both AD + AC and MW + AC samples after 72 h. In particular, the MW + AC sample surfaces indicated the highest cell attachment and growth compared to the other groups.

The trends for DNA content, which is typically used as a measure of total cell number, were generally similar to those of the MTT data with the exception that there was no significant increase in DNA content in cells cultured on the MW + AC surface. Total DNA levels in the cells were similar across all four surface treatments and both time points (Figure 6), indicating similar biological behaviors and the development of a stable (nondividing) cell monolayer by 2 weeks postseeding.

Figure 7 shows the osteocalcin production from cells growing on the various sample surfaces as an indicator of osteogenic maturation. The data were normalized with respect to the total DNA content to more accurately assess the differentiation of viable cells in the culture. At 2 weeks, the MW + AC sample group showed significantly higher osteocalcin expression compared to all other groups ($p < 0.001$). Although there was an increase in OC production in the AD + AC group, this difference was not statistically significant.

The data shown in Figure 8 represents the osteoblastic mineralization across the various sample types. Alizarin Red S content was significantly higher in the AD + AC and MW + AC groups than in either the uncoated PEEK or the AD samples. A small increase in mineralization was observed in the AD samples as compared to the PEEK sample group; however, it was not statistically significant.

DISCUSSION

Ion beam sputtering with secondary ion bombardment proved to be an effective method for depositing a 2-μm dual-layer HA/YSZ coating with high density on PEEK. The coatings show that YSZ exhibits crystalline properties while HA is amorphous in the as-deposited state, evident by SEM and XRD. Microwave heat treatment of the coatings resulted in crystallization of the HA layer at sub-critical temperatures for PEEK damage as shown by SEM and XRD. The underlying crystal structure of the YSZ layer, in addition to heat protection, was also shown to provide nucleation sites for crystal growth of the HA layer during heat treatment, reducing the energy needed for initiation. This is supported by the crystal growth observed in Figure 2(b), where crystalline structures are present at the HA/YSZ interface as well as the top surface. Crystallization at the top surface is expected due to the nature of the autoclave treatment process, which heats the material from the outer

Author Manuscript Author Manuscript Author Manuscript Author Manuscript

surface. The unexpected initiation and growth observed at the interface supports the presence of nucleation sites at the YSZ surface. Conversely, microwave heating is a volumetric process, and thus crystallization is distributed more evenly throughout the layer thickness as in Figure 2(c).

The FTIR analysis shows the absence of the hydroxyl group in the HA coating, and postdeposition treatments (AD + AC, MW + AC) did not have a noticeable effect on the presence of the hydroxyl group. This is a common phenomenon in films containing low-density elements deposited using vacuum sputtering units.[20]

The *in vitro* study was performed to determine the biological response to the coated samples as compared to the uncoated PEEK. Uncoated PEEK was chosen as a control in this study as it is what is currently available to surgeons as a clinical implant material for spinal implants. The MC3T3 cell line was selected for study as it is a stable and well-characterized osteoblastic cell line that undergoes biologically relevant differentiation and mineralization *in vitro*.

The data from the MTT assay indicated that all sample surfaces provided a suitable environment for cell viability, while crystalline HA sample surfaces had a positive effect on cell proliferation. It was observed that MW + AC samples had the most promising short-term cellular response. The DNA content results at 2- and 3-week intervals showed very little change in number of viable cells. A plateau in total DNA was expected with these cells beyond 10–14 days under normal conditions, and showed that the surfaces supported cell proliferation and the development of a stable confluent monolayer. The normalized osteocalcin results reveal the rate of differentiation on the MW + AC surface supports quick osteogenic maturation as evident from the high levels of osteocalcin observed at 2- and 3-week periods. Increased differentiation was observed for the AD and AD + AC coated groups from 2 to 3 weeks while the PEEK remained mostly unchanged and by 3 weeks, both AD + AC and MW + AC coated groups exhibited the highest osteocalcin synthesis. This is likely due to an increased cell affinity for the crystalline HA surface. The mechanisms underlying the response of cells to different surface coatings are likely quite complex. Certainly it is well recognized that cells respond differentially to differences in physicochemistry,[21] including alterations in surface topography,[22,23], surface chemistry,[24] and surface charge. The significance of these parameters in this study is unclear, but it appears that the crystalline region at the top surface of AD + AC samples seemed to exhibit a similar biological response to the more crystallized MW + AC treated samples. The enhanced crystallinity in the MW + AC samples may play an even more significant role in determining the long-term response to the implant, an issue that can only be fully answered through *in vivo* testing in an appropriate animal model.

The Alizarin Red S staining results show calcium deposits formed by the osteoblasts via mineralization on the sample surfaces. There was an order of magnitude increase in mineralization in the AD + AC and MW + AC samples compared with uncoated PEEK and AD samples, demonstrating the ability of the crystalline HA coatings to support and accelerate new bone formation. An *in vivo* animal study is ongoing to further investigate the biological response to the HA/YSZ coating on an implanted PEEK device.

Author Manuscript Author Manuscript Author Manuscript Author Manuscript

CONCLUSIONS

In this study, IBAD was successfully used to deposit HA/YSZ coatings on PEEK substrates. The HA coating layer was heat-treated to induce crystallization from its amorphous state without damaging the underlying polymer. The *in vitro* study showed that crystalline HA/YSZ coatings supported osteoblastic differentiation, and accelerated osteogenic maturation and bone growth. In particular, coatings that underwent microwave plus autoclave heat treatment exhibited superior bioactivity and may offer significant enhancements for implantable PEEK biomaterials.

Acknowledgments

Contract grant sponsor: National Institute of Dental and Craniofacial Research of the National Institutes of Health; contract grant number: R21DE022925

The content is solely the responsibility of the authors and does not necessarily represent the official views of the National Institutes of Health.

References

1. Bauer TW, Schils J. The pathology of total joint arthroplasty. Skeletal Radiol. 1999; 28:483–497. [PubMed: 10525792]
2. Ramakrishna S, Mayer J, Wintermantel E, Leong KW. Biomedical applications of polymer-composite materials: a review. Compos Sci Technol. 2001; 61:1189–1124.
3. Kurtz SM, Devine JN. PEEK biomaterials in trauma, orthopedic, and spinal implants. Biomaterials. 2007; 28:4845–4869. [PubMed: 17686513]
4. Eschbach L. Nonresorbable polymers in bone surgery. Injury. 2000; 31(Supplement 4):D22–D27.
5. Godara A, Raabe D, Green S. The influence of sterilization processes on the micromechanical properties of carbon fiber-reinforced PEEK composites for bone implant applications. Acta Biomater. 2007; 3:209–220. [PubMed: 17236831]
6. Toth JM, Wang M, Estes BT, Scifert JL, Seim HB III, Turner AS. Polyetheretherketone as a biomaterial for spinal applications. Bio-materials. 2006; 27:324–334.
7. Ferguson SJ, Visser JMA, Polikeit A. The long-term mechanical integrity of non-reinforced PEEK-OPTIMA polymer for demanding spinal applications: Experimental and finite-element analysis. Eur Spine J. 2005; 15:149–156. [PubMed: 15940477]
8. Martin BI, Mirza SK, Comstock BA, Gray DT, Kreuter W, Deyo RA. Reoperation rates following lumbar spine surgery and the influence of spinal fusion procedures. Spine. 2007; 32:382–387. [PubMed: 17268274]
9. Briem D, Strametz S, Schröoder K, Meenen NM, Lehmann W, Linhart W, Ohl A, Rueger JM. Response of primary fibroblasts and osteoblasts to plasma treated polyetheretherketone (PEEK) surfaces. J Mater Sci Mater Med. 2005; 16:671–677. [PubMed: 15965600]
10. Sun L, Berndt CC, Gross KA, Kucuk A. Material fundamentals and clinical performance of plasma-sprayed hydroxyapatite coatings: A review. J Biomed Mater Res. 2001; 58:570–592. [PubMed: 11505433]
11. Almasi D, Izman S, Assadian M, Ghanbari M, Abdul Kadir MR. Crystalline ha coating on peek via chemical deposition. Appl Surf Sci. 2014; 314:1034–1040.
12. Hahn B-D, Park D-S, Choi J-J, Ryu J, Yoon W-H, Choi J-H, Kim J-W, Ahn C-W, Kim H-E, Yoon B-H, Jung I-K. Osteoconductive hydroxyapatite coated PEEK for spinal fusion surgery. Appl Surf Sci. 2013; 283:6–11.
13. Barkarmo S, Wennerberg A, Hoffman M, Kjellin P, Breding K, Handa P, Stenport V. Nano-hydroxyapatite-coated PEEK implants: A pilot study in rabbit bone. J Biomed Mater Res A. 2013; 101A:465–471.

Author Manuscript Author Manuscript Author Manuscript Author Manuscript

14. Rabiei A, Sandukas S. Processing and evaluation of bioactive coatings on polymeric implants. J Biomed Mater Res A. 2013; 101A:2621–2629.
15. Muralithran G, Ramesh S. The effects of sintering temperature on the properties of hydroxyapatite. Ceram Int. 2000; 26:221–230.
16. Ozeki K, Aoki H, Masuzawa T. Influence of the hydrothermal temperature and pH on the crystallinity of a sputtered hydroxyapatite film. Appl Surf Sci. 2010; 256:7027–7031.
17. Bai X, Sandukas S, Appleford MR, Ong JL, Rabiei A. Deposition and investigation of functionally graded calcium phosphate coatings on titanium. Acta Biomater. 2009; 5:3563–3572. [PubMed: 19463973]
18. Blalock T, Bai X, Rabiei A. A study on microstructure and properties of calcium phosphate coatings processed using ion beam assisted deposition on heated substrates. Surf Coat Technol. 2007; 201:5850–5858.
19. Rabiei, A. Processing of biocompatible coating on polymeric implants [Internet]. 2012. [cited 2015 Apr 28]. Available from: http://www.google.com/patents/US8323722
20. Yang Y, Kim K-H, Mauli Agrawal C, Ong JL. Effect of post-deposition heating temperature and the presence of water vapor during heat treatment on crystallinity of calcium phosphate coatings. Biomaterials. 2003; 24:5131–5137. [PubMed: 14568429]
21. Wang J, de Boer J, de Groot K. Proliferation and differentiation of osteoblast-like MC3T3-E1 cells on biomimetically and electrolytically deposited calcium phosphate coatings. J Biomed Mater Res A. 2009; 90:664–670. [PubMed: 18563812]
22. Li N, Chen G, Liu J, Xia Y, Chen H, Tang H, Zhang F, Gu N. Effect of surface topography and bioactive properties on early adhesion and growth behavior of mouse preosteoblast MC3T3-E1 cells. ACS Appl Mater Interfaces. 2014; 6:17134–17143. [PubMed: 25211771]
23. Wu C, Chen M, Zheng T, Yang X. Effect of surface roughness on the initial response of MC3T3-E1 cells cultured on polished titanium alloy. Biomed Mater Eng. 2015; 26(Suppl1):S155–S164. [PubMed: 26405920]
24. Keselowsky BG, Collard DM, García AJ. Integrin binding specificity regulates biomaterial surface chemistry effects on cell differentiation. Proc Natl Acad Sci USA. 2005; 102:5953–5957. [PubMed: 15827122]

Author Manuscript Author Manuscript Author Manuscript Author Manuscript

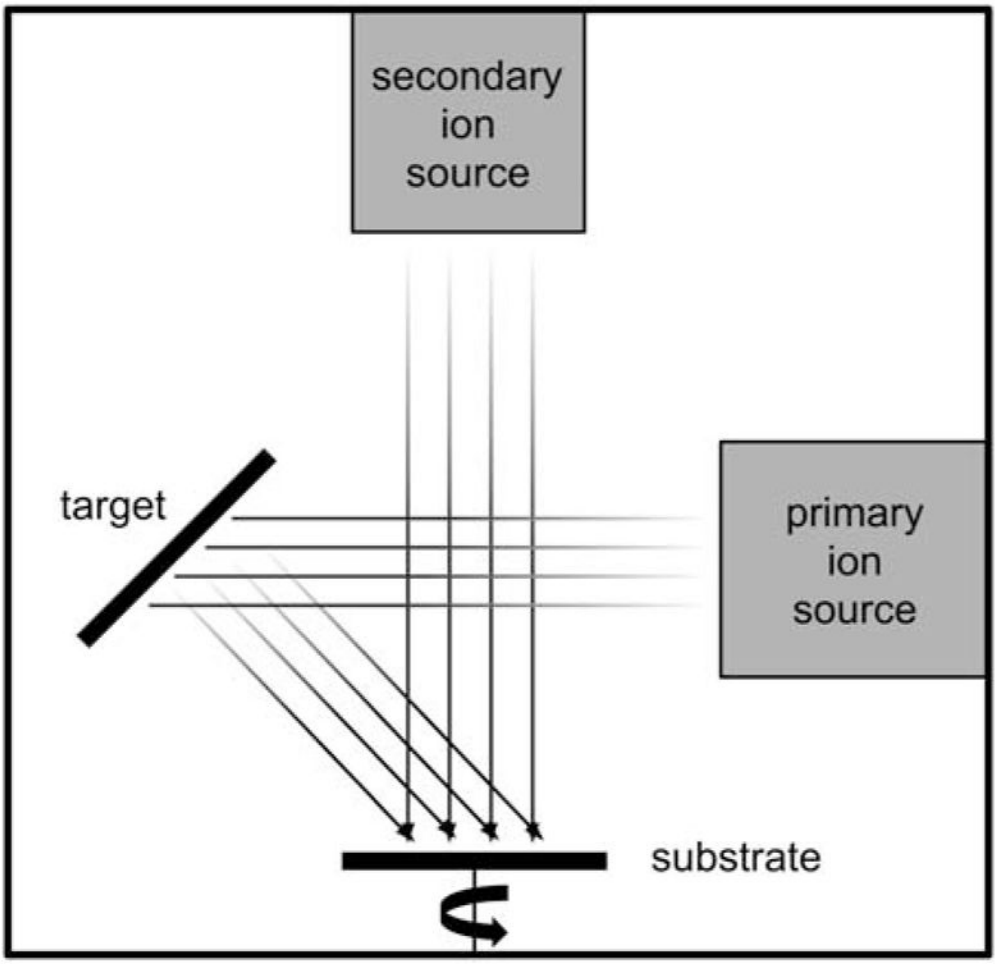

FIGURE 1.
Schematic drawing of ion-beam-assisted deposition (IBAD) system.

Author Manuscript Author Manuscript Author Manuscript Author Manuscript

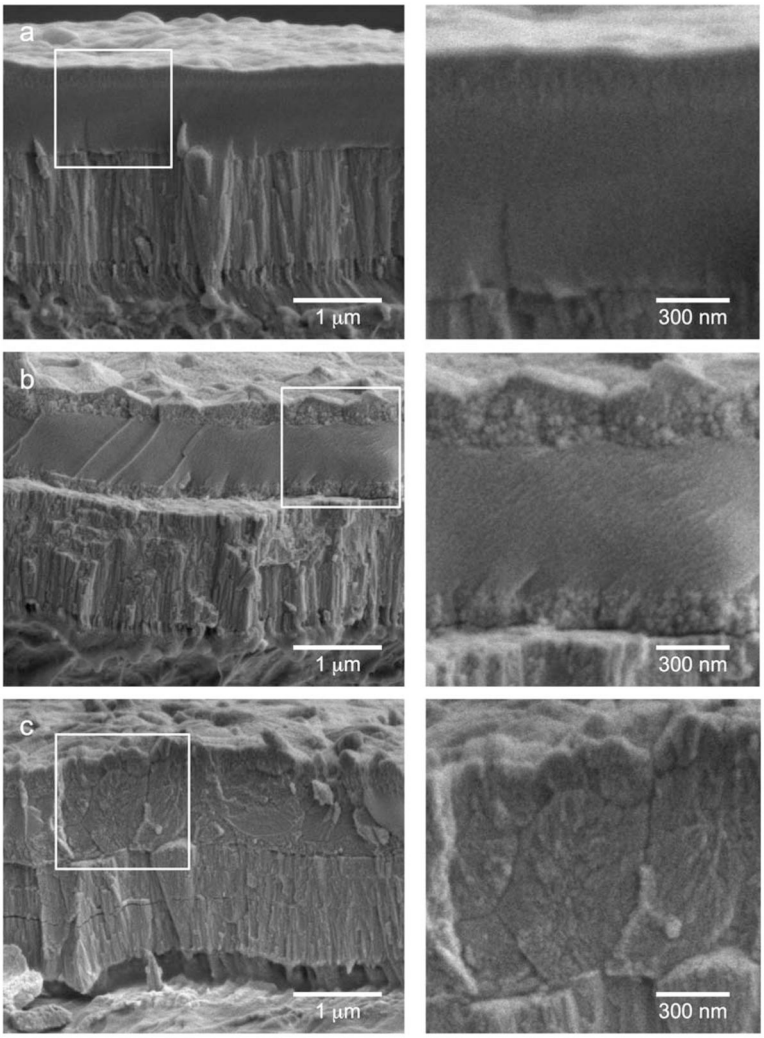

FIGURE 2.

SEM images of the cross-sections of (a) AD, (b) AD + AC, and (c) MW + AC coatings. Inscribed boxes show location of magnified view of HA layer (right side).

Author Manuscript Author Manuscript Author Manuscript Author Manuscript

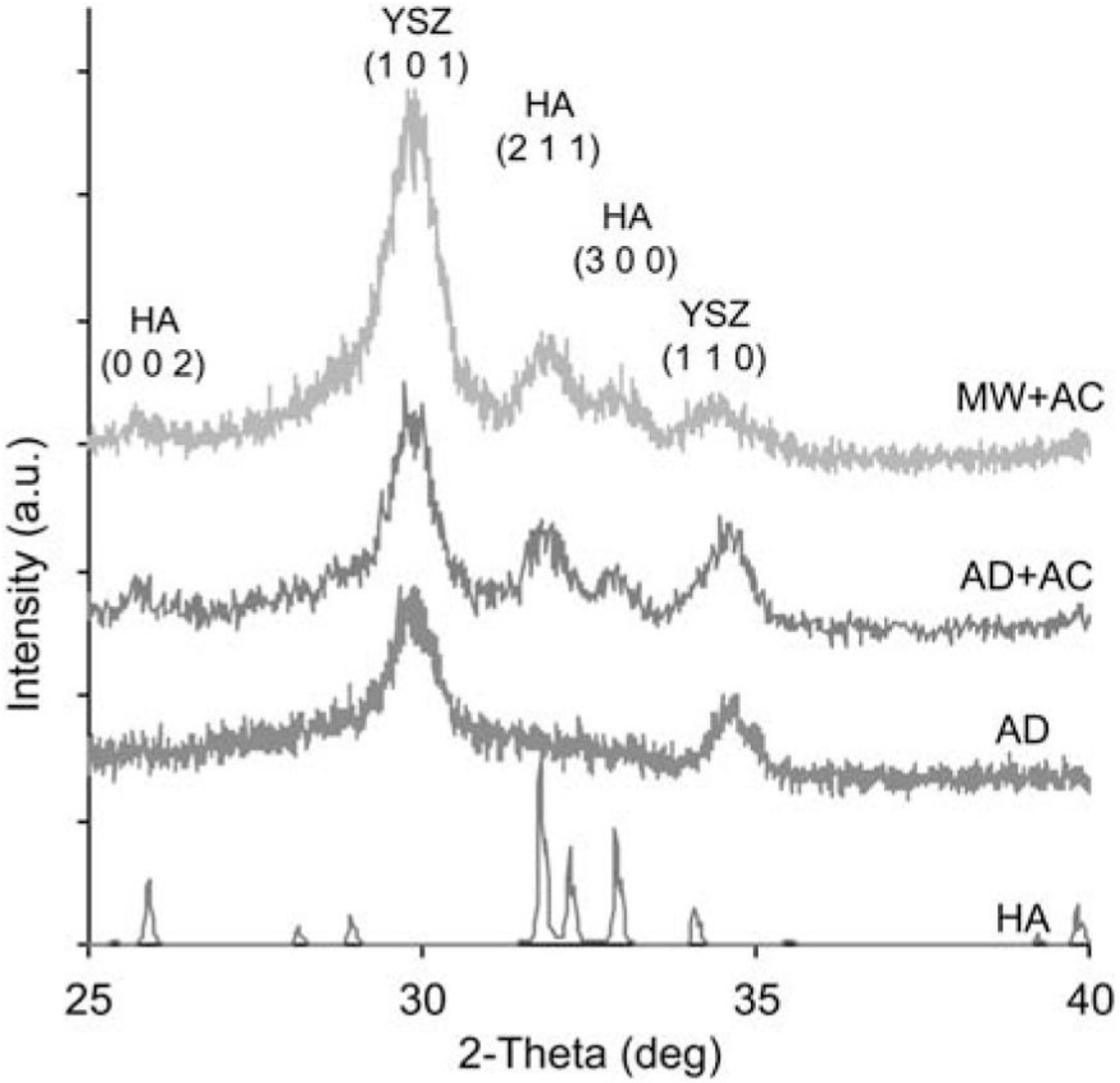

FIGURE 3.

XRD data of HA target and HA/YSZ coatings as-deposited (AD), autoclave treated (AD + AC), and microwave plus autoclave treated (MW + AC). Standard peak locations are indicated for YSZ and HA phases. [Color figure can be viewed in the online issue, which is available at wileyonlinelibrary.com.]

Author Manuscript Author Manuscript Author Manuscript Author Manuscript

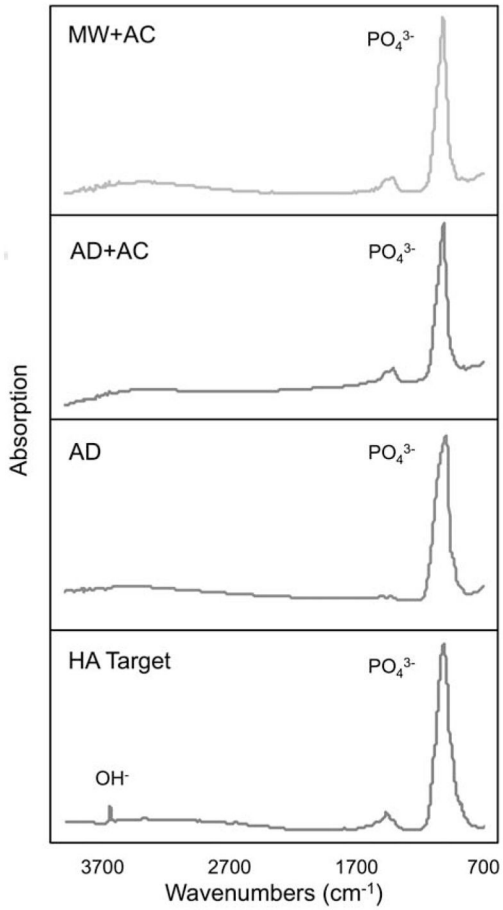

FIGURE 4.

FTIR spectra of HA target and HA/YSZ coatings as-deposited (AD), autoclave treated (AD + AC), and microwave plus autoclave treated (MW + AC). [Color figure can be viewed in the online issue, which is available at wileyonlinelibrary.com.]

Author Manuscript Author Manuscript Author Manuscript Author Manuscript

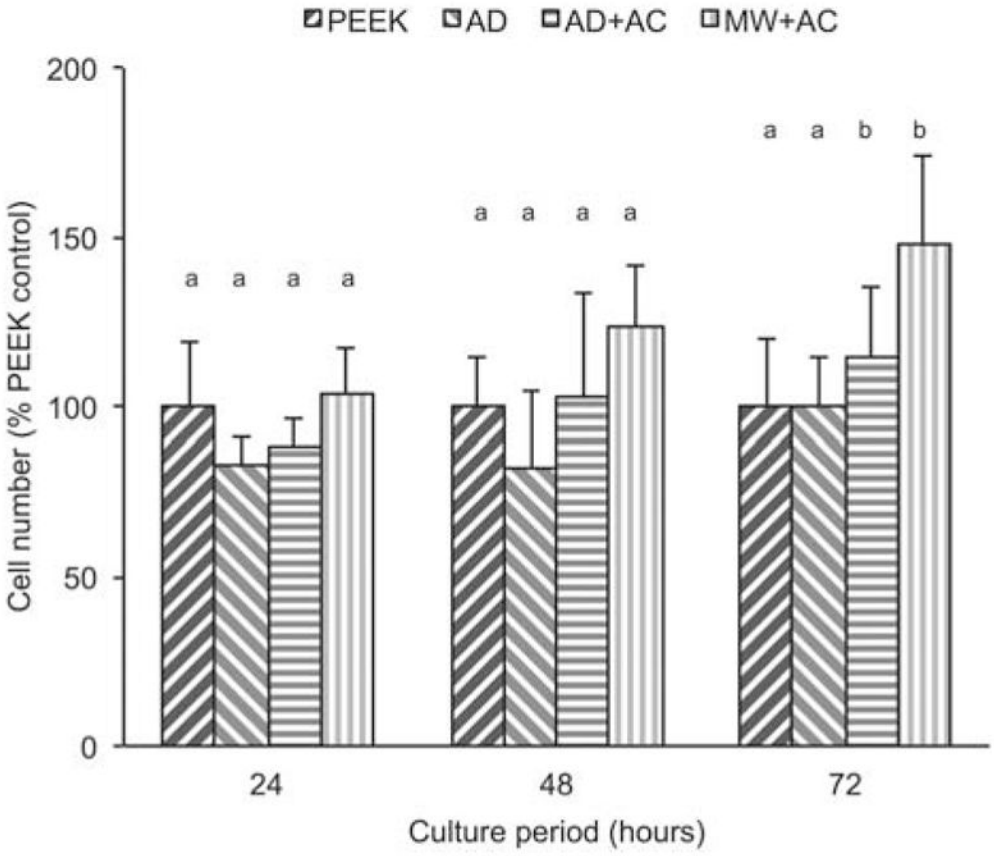

FIGURE 5.

MTT assay results at various time points for uncoated PEEK (PEEK), as-deposited (AD), autoclave treated (AD + AC), and microwave plus autoclave treated (MW + AC). Statistically similar groups indicated by group (a, b, and so forth). [Color figure can be viewed in the online issue, which is available at wileyonlinelibrary.com.]

Author Manuscript Author Manuscript Author Manuscript Author Manuscript

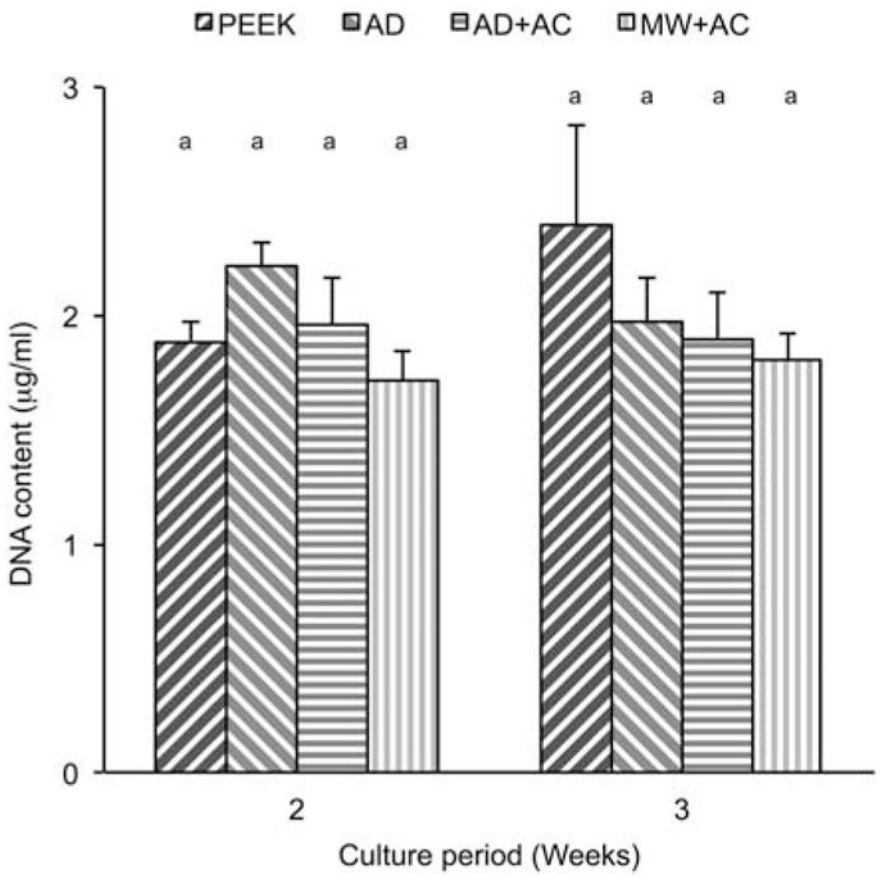

FIGURE 6.

DNA content results at various time points for uncoated PEEK (PEEK), as-deposited (AD), autoclave treated (AD + AC), and microwave plus autoclave treated (MW + AC). Statistically similar groups indicated by group (a, b, and so forth). [Color figure can be viewed in the online issue, which is available at wileyonlinelibrary.com.]

Author Manuscript Author Manuscript Author Manuscript Author Manuscript

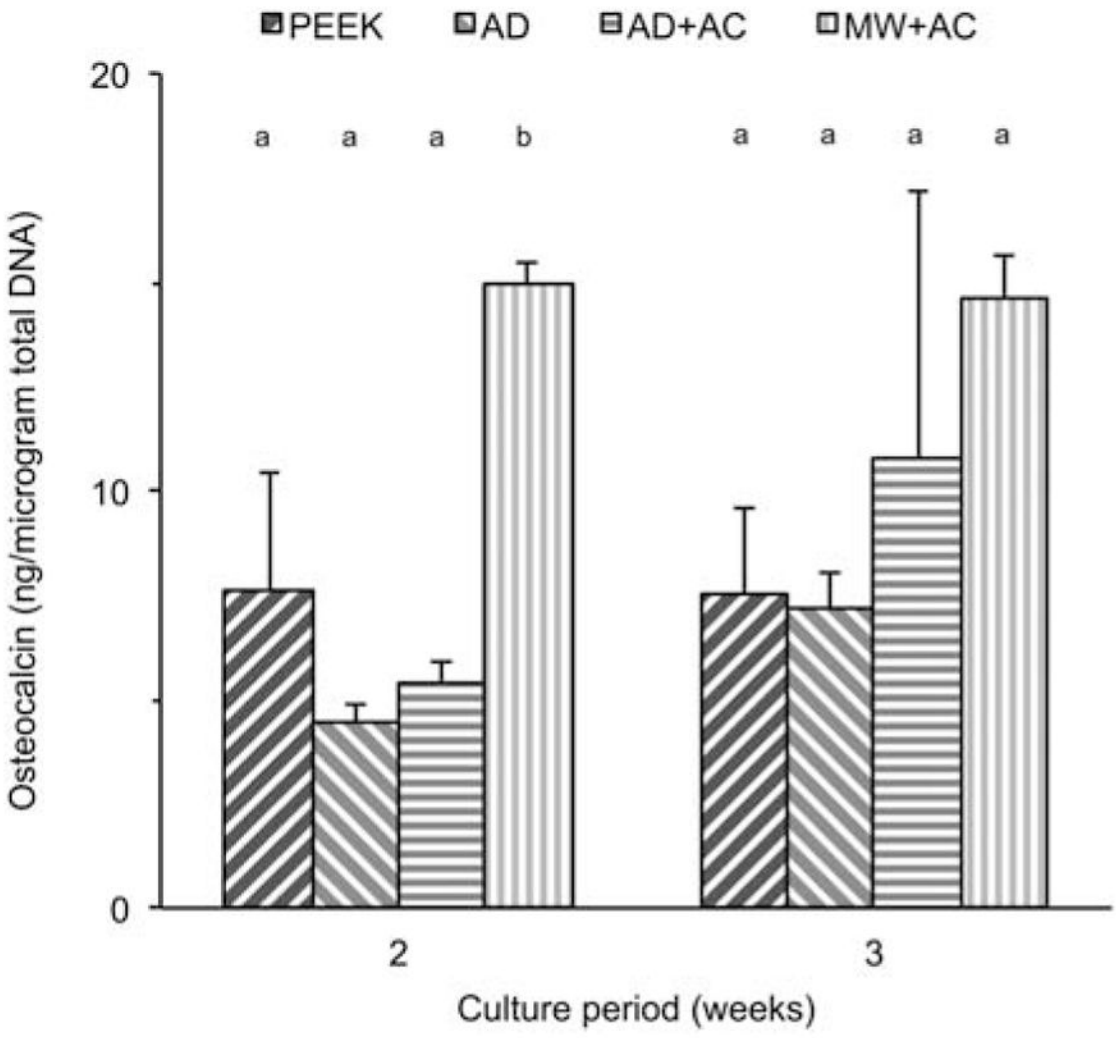

FIGURE 7.

Normalized osteocalcin results at various time points for uncoated PEEK (PEEK), as-deposited (AD), autoclave treated (AD + AC), and microwave plus autoclave treated (MW + AC). Statistically similar groups indicated by group (a, b, and so forth). [Color figure can be viewed in the online issue, which is available at wileyonlinelibrary. com.]

Author Manuscript Author Manuscript Author Manuscript Author Manuscript

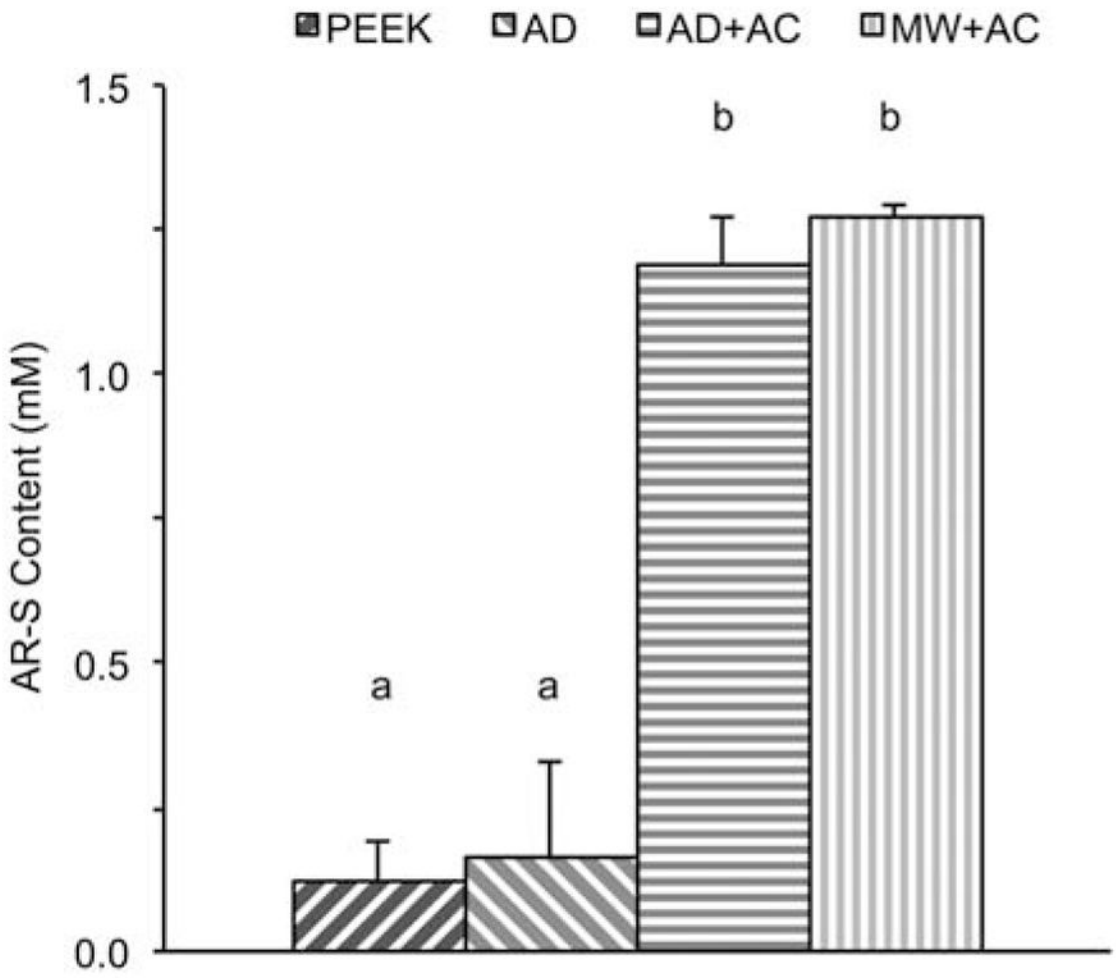

FIGURE 8.

Biomineralization results shown by Alizarin Red-S content for uncoated PEEK (PEEK), as-deposited (AD), autoclave treated (AD + AC), and microwave plus autoclave treated (MW + AC). Statistically similar groups indicated by group (a, b, and so forth). [Color figure can be viewed in the online issue, which is available at wileyonlinelibrary.com.]